

Photoreflectance and photoluminescence investigations of a step-like GaInNAsSb/GaNAs/GaAs quantum well tailored at 1.5 μm : The energy level structure and the Stokes shift

R. Kudrawiec^{a)}

Institute of Physics, Wrocław University of Technology, Wybrzeże Wyspińskiego 27, 50-370 Wrocław, Poland

H. B. Yuen

Solid State and Photonics Laboratory, Department of Electrical Engineering, 126X CISX, Via Ortega, Stanford University, Stanford, California 94305-4075

K. Ryczko and J. Misiewicz

Institute of Physics, Wrocław University of Technology, Wybrzeże Wyspińskiego 27, 50-370 Wrocław, Poland

S. R. Bank, M. A. Wistey, H. P. Bae, and James S. Harris, Jr.

Solid State and Photonics Laboratory, Department of Electrical Engineering, 126X CISX, Via Ortega, Stanford University, Stanford, California 94305-4075

(Received 27 August 2004; accepted 7 December 2004; published online 15 February 2005)

The energy level structure of a step-like GaInNAsSb/GaNAs/GaAs quantum well (QW) has been investigated by photoreflectance (PR) spectroscopy and was analyzed by theoretical calculations. In the active region of this structure, i.e., GaInNAsSb/GaNAs QW, we have observed PR resonances related higher order QW transitions in addition to the ground state transition. Based on calculations from experimental data, we have found that the electron effective mass in the active QW is $0.12m_0$ and the conduction band offset for GaInNAsSb/GaAs interface is about 0.85. The emission observed from this structure at 10 K has a small Stokes shift (i.e., 6 meV and <2 meV for as-grown and annealed structures, respectively) and is without the exponential-like tail at the low-energy side. Hence, we conclude that the incorporation of Sb atoms into GaInNAs alloy helps to achieve QW structures which emit light at longer wavelength and have quite narrow emission line and small Stokes shift. © 2005 American Institute of Physics. [DOI: 10.1063/1.1854729]

I. INTRODUCTION

Semiconductor lasers operating at 1.3 and 1.55 μm wavelengths are very important light sources for fiber telecommunication. In 1996, Kondow proposed GaInNAs/GaAs quantum well (QW) as a novel GaAs-based material system for this application.¹ GaInNAs-based lasers grown on GaAs substrates offer a number of advantages in comparison with current GaInAsP-based lasers grown on InP substrates. The GaInNAs/GaAs system has a larger conduction band discontinuity and therefore provides better electron confinement and characteristic temperature. Moreover, this system is compatible with the well developed GaAs/AlAs distributed Bragg reflectors for surface emitting sources and AlAs oxide current confinement techniques. From an economic perspective, GaInNAs-based lasers use the cheaper and more robust GaAs substrate as compared to the more expensive and fragile InP substrate used in GaInAsP-based lasers. Nowadays, the GaInNAs/GaAs lasers present very competitive characteristics at 1.3 μm wavelength,^{2–11} but it remains difficult to obtain comparable performance at longer emission wavelengths. With increasing nitrogen concentration, especially above 2.5%, the optical quality of the material usually dete-

riorates significantly resulting in a higher threshold current density of lasers. Therefore, the nitrogen containing structures are often annealed because it significantly enhances photoluminescence (PL) intensity. Annealing, however, has the disadvantage in which the band gap energy blueshifts.^{12–15} Optimal values which are typically used for 1.3 μm emission are, respectively, $\sim 35\%$ In and $\sim 1\%$ N. Higher In compositions increase the compressive strain past a critical point in which the QW structural quality is degraded. Higher nitrogen composition introduces nonradiative centers which results in poor optical properties. For these reasons, other approaches were developed to redshift the emission wavelength and maintain good optical quality.¹⁶ One of them is to introduce strain compensated Ga(In)NAs layers to this GaInNAs/GaAs QW structure,^{17–24} the active region of such a laser structure is a step-like QW. The other approach is to incorporate Sb atoms into GaInNAs compound.^{25–36} It has been found that the incorporation of Sb atoms into GaInNAs, besides a lowering of the band gap energy, significantly improves the structural and optical properties of this compound.^{27,30} Combining the idea of step-like QW structure with the active region consisting of GaInNAsSb/GaNAs quantum well seems to be one of the most appropriate approaches to obtain long-wavelength lasers. Recently, a 1.46 μm vertical-cavity surface-emitting laser (VCSEL) grown on GaAs substrate with the

^{a)}Author to whom correspondence should be addressed; electronic mail: robert.kudrawiec@pwr.wroc.pl

GaInNAsSb/GaNAs QW has been reported.³⁴ In order to tailor the most optimum structures, experimental data about band gap discontinuities for this system are necessary. So far, the knowledge about the energy level structure for GaInNAsSb/GaNAs QW systems is unknown. An investigation of the number of confined states for electrons and holes and the energy difference between them is a very interesting task. Photorefectance (PR) spectroscopy is an excellent technique to investigate both the fundamental and higher order QW transitions.^{37,38} The simulation of PR data with theoretical calculations makes it possible to determine material parameters like the band gap discontinuity. Such procedures have often been applied in different semiconductor structures.^{37–42}

In this article we study a step-like GaInNAsSb/GaNAs/GaAs QW structure very similar to this one reported in Refs. 31 and 34. In order to determine the energy level structure and band gap discontinuities, we applied PR spectroscopy supported by theoretical calculations. The effect of postgrowth annealing has also been investigated in this article. We have determined the Stokes shift for the as-grown and annealed structure by measuring PR and PL at 10 K.

II. EXPERIMENT

The step-like GaInNAsSb/GaNAs/GaAs QW structure was grown by solid-source molecular beam epitaxy on semi-insulating GaAs substrates. The sample is composed of 250-nm-thick GaAs buffer layer, 50-nm-thick GaAs:N layer with the nitrogen concentration of $\sim 0.1\%$, GaNAs step-like barriers, GaInNAsSb QW, and 50-nm-thick GaAs cap layer. The GaInNAsSb/GaNAs QW has a nominal composition of 39% In, 1.7% N, 2% Sb in the GaInNAsSb layer and 2.7% N in the GaNAs barriers. The nominal thickness of the GaNAs step-like barriers and GaInNAsSb QW is 20 and 7.5 nm, respectively. In addition, a sample without GaInNAsSb QW was grown as a reference structure useful in the interpretation of PR spectra for the step-like QW structure. The GaAs:N layer is not an intentional part of the structure, but a result of the growth method we use. Other details of the growth conditions can be found in Refs. 27, 29–32, and 34. A piece of the step-like QW structure was annealed at 760 °C for 60 s.

The PR experiment was performed with a tungsten halogen lamp (150 W) as a probe light source. For photomodulation, a 532 nm line of a yttrium–aluminum–garnet (YAG) laser with 15 mW power was used as a pump beam that was mechanically chopped at a frequency of 285 Hz. The probe and pump beams were defocused to the diameter of 5 mm. A single grating 0.55 m monochromator and a thermoelectrically cooled GaInAs *p-i-n* photodiode were used to analyze the reflected light. Other details of the PR setup can be found elsewhere.³⁸ Photoluminescence experiment was performed with the same monochromator and laser. The excitation beam was focused onto sample that excitation power density was about ~ 50 mW/cm².

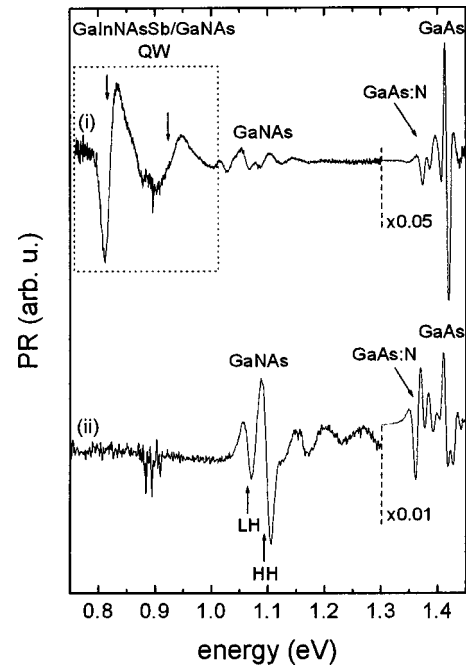


FIG. 1. Room temperature photorefectance spectra of as-grown step-like GaInNAsSb/GaNAs/GaAs QW structure (i) and GaNAs/GaAs structure (ii).

III. RESULTS

Figure 1 shows room temperature PR spectra of the step-like GaInNAsSb/GaNAs/GaAs QW structure [curve (i)] and the reference GaNAs/GaAs structure [curve (ii)]. In the case of the reference structure, PR features associated with the absorption in GaNAs, GaAs:N, and GaAs layers are clearly observed. PR features related to GaNAs layer are composed of two resonances associated with absorption between the light- (heavy-) hole band and the electron band. The light-hole (LH) transition is at lower energy than heavy-hole (HH) transition due to the tensile strain in this layer. The signal between PR resonances attributed to GaNAs and GaAs:N layers is also associated with the GaNAs layer. The origin of this signal could be a weak built-in electric field in the structure, because the signal looks like Franz–Keldysh oscillations.^{37,38,43} The other origin of this signal could be absorption between higher order subbands in the GaNAs/GaAs system as has been shown in Ref. 44. However, in this article we do not consider this part of PR spectrum in detail.

All PR features observed for the reference sample are also observed for the step-like GaInNAsSb/GaNAs/GaAs QW structure but they are not discussed in this article in detail. In this work we focus on PR features related to absorption in the active part of the laser structure, i.e., in the GaInNAsSb/GaNAs QW. PR resonances associated with the absorption in the GaInNAsSb/GaNAs QW are clearly observed below 1.05 eV. We can identify two resonances at energies ~ 0.82 and ~ 0.93 eV. An additional resonance between the two main resonances is also visible. Unfortunately, the noise associated with an absorption related to H₂O appears at this energy (see also the reference sample). In order

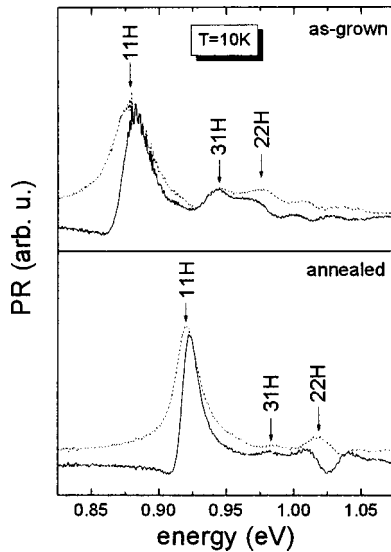


FIG. 2. Photorefectance spectra (solid lines) measured at 10 K for as-grown (a) and annealed GaInNAsSb/GaNAs/GaAs QW structure (b) together with Kramers–Kronig modulus (dashed lines).

to clarify the number of QW transitions and determine particular QW levels, we have measured PR at low temperatures.

Figures 2(a) and 2(b) show low-temperature PR spectra of the as-grown and annealed step-like QW structures, respectively. The dashed lines in Fig. 2 are the moduli of PR spectra obtained by Kramers–Kronig analysis (KKA) of PR spectra.^{45,46} This analysis, besides the standard fitting procedure,³⁷ helps identify optical transitions observed in PR spectra. With the decrease of temperature, the PR lines narrow and shift to higher energies. This facilitates a more careful identification of the number of PR resonances and their oscillator strengths. Finally, we have identified two strong PR resonances related to 11H and 22H transitions and one weaker related to 31H transition. The notation nmH denotes the transition between n th heavy-hole valence subband and m th conduction subband. Such identification of the resonances is consistent with the selection rules for square-like QWs and agrees with the theoretical calculations for this system. The last argument could be controversial due to poor knowledge of the parameters for the GaInNAsSb alloy. However, the careful analysis of an acceptable spectrum of parameters for this material system leads to the conclusion that two states are confined in the electron QW and three states are confined in the heavy-hole QW. Details of our analysis are presented below. We decided to calculate and analyze carefully the data at room temperature due to the better knowledge of material parameters for this system at this temperature. Also, we limited our considerations to the as-grown structure. In the case of annealed QW structure, only a shift of QW transitions is expected without a change in the number of confined states. The shift could be associated with both (i) a blueshift of GaInNAsSb band gap energy and (ii) a phenomenon of the atom interdiffusion across GaInNAsSb/GaNAs interfaces.⁴⁷ We suppose that in our samples the second effect is less important than the first one as in GaInNAs/GaAs QW systems.^{47–49} Therefore, the en-

tirety of the blueshift found in the GaInNAsSb/GaNAs QW structure (~ 42 meV) is attributed to the blueshift of band gap energy of GaInNAsSb layer. The effect of the blueshift of band gap energy due to the postgrowth annealing is typical of all dilute-nitride alloys.^{47–52} In the case of this alloy, almost all the blueshift is associated with a change in nitrogen nearest-neighbor environment from Ga-rich to In-rich environments of N atoms.^{51,52} However, the blueshift of band gap energy has also been observed for GaNAs and GaNAsSb alloys, i.e., In free alloys.^{15,50} In this case, the blueshift phenomenon cannot be explained by the effect of short range ordering like that in GaInNAs. The blueshift is attributed to the annealing-induced reduction of the tail of density of states.^{15,51} Finally, we assume that for GaInNAsSb alloy, both the change in nitrogen nearest-neighbor environments and the reduction of the tail of density of states are important and lead to the blueshift of band gap energy.

The calculations of QW energy levels were performed within the framework of the usual envelope function approximation.⁵³ The excitonic effect was neglected. In order to find the band gap energy for GaNAs and GaInNAsSb layers, we have adopted the band anticrossing (BAC) model with typical parameters: $E_N=1.65$ eV, and $C_{NM}=2.7$ eV.⁵⁴ According to the BAC model, the influence of nitrogen localized states on the valence band structure is neglected. Hence, we have assumed that the effective mass of light and heavy hole does not change after adding nitrogen atoms. The biaxial strain was calculated based on the Pikus–Bir Hamiltonian⁵⁵ as in Ref. 56. The energy shifts due to hydrostatic δE_H and shear δE_S strain components equal

$$\delta E_H = 2a \left(1 - \frac{C_{12}}{C_{11}} \right) \varepsilon, \quad (1)$$

$$\delta E_S = b \left(1 + 2 \frac{C_{12}}{C_{11}} \right) \varepsilon, \quad (2)$$

where ε is the strain tensor in the plane of the interfaces, C_{11} and C_{12} are elastic stiffness constants, and a and b are the hydrostatic and shear deformation potentials, respectively. All the parameters have been obtained by linear interpolation between the parameters of a relevant binary semiconductor.⁵⁷ In our calculations, we consider m_e^* and Qc as free parameters. However, we have limited the range of the two parameters on the basis of literature data.^{58–66} We assume the electron effective mass to be in the range of 0.06–0.3 m_0 . In our calculations, we do not assume the Qc parameter for the GaInNAsSb/GaNAs interface directly. We consider independently the Qc parameter for both GaNAs/GaAs and GaInNAsSb/GaAs interfaces. In our calculations we limited Qc parameter to 0.75–1.0 for GaNAs/GaAs interface and to 0.6–1.0 for GaInNAsSb/GaAs interface. However, if we assume that GaInNAsSb/GaNAs QW is type I, we automatically limit the possible Qc to a narrower range because, for some Qc , we obtain quantum confinement in the barrier for electrons instead of the QW, e.g., the case of $Qc=1.0$ and $Qc=0.75$ for GaNAs/GaAs and GaInNAs/GaAs interfaces, respectively. In the case of the valence band, strains present in our sample ($\varepsilon=-0.55\%$ for GaNAs and $\varepsilon=2.61\%$ for

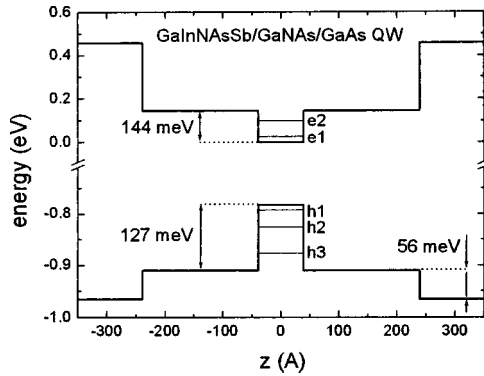


FIG. 3. Band diagram of the step-like GaInNAsSb/GaNAs/GaAs QW structure obtained on the basis of the matching of theoretical calculations with experimental data. This diagram has been obtained for the following parameters: $Q_c=0.8$ for GaInNAsSb/GaAs and $Q_c=0.85$ for GaInNAsSb/GaNAs interfaces; $m_e=0.12m_0$.

GaNAsSb) lead to the structure of type I and II for heavy and light holes, respectively. Therefore, all PR resonances related to absorption in GaInNAsSb/GaNAs QW are attributed to transitions between heavy-hole and electron subbands. Some indirect transitions between light holes confined in GaNAs step-like barriers and the first electron subband are also possible, however, due to weak overlap of the electron and hole wave functions, such transitions are neglected in our analysis. Important parameters in the calculations are the QW width and the content of QW and barriers. The first influences energies of QW transitions and energy differences between them while the second influences mainly energies of QW transitions. The width of QW was verified to be 7.8 nm by high-resolution x-ray diffraction (HRXRD). The content of GaInNAsSb and GaNAs layers was determined by secondary ion mass spectroscopy and HRXRD measurements as being close to the nominal values. Details of the calibration steps are described elsewhere.^{27,30} Therefore our calculations do not vary the nominal content for both the QW and barriers especially, that the BAC parameters for GaInNAsSb alloy are unknown. We have assumed that the best solution is to adjust C_{MN} parameter to such a value for which the energy of the ground state transition agrees with experimental value. Finally, for the calculations presented in this article we have assumed that C_{MN} is 2.5 eV.

The band diagram for the as-grown step-like QW structure obtained on the basis of matching theoretical calculations with experimental data obtained at room temperature is shown in Fig. 3. In this case, we obtained that the depth of electron and heavy-hole QW is ~ 144 and ~ 127 meV, respectively. The depth of the wells results from the Q_c for GaNAs/GaAs and GaInNAsSb/GaAs interfaces and strain effects. Note that in our calculations, we assume Q_c before taking into account the strain effects. In the case of low Q_c for GaNAs/GaAs interface, we obtained only one electron state in GaInNAsSb/GaNAs QW. We had tried to match the result with experimental data; however, the energy differences between PR resonances are much larger than calculated values. Hence, we conclude that we have to have two confined states for electrons. This leads to a strong correlation between Q_c for GaNAs/GaAs and GaInNAsSb/GaAs

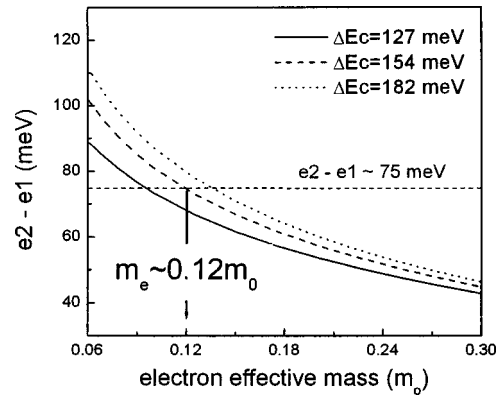


FIG. 4. The energy difference between the second and the first electron level vs the electron effective mass. Calculations were performed for different depths of the electron QW, i.e., different band gap alignments. The solid, dashed and dotted lines correspond to $Q_c=0.8, 0.85,$ and $0.9,$ for GaInNAsSb/GaAs interface, respectively, at $Q_c=0.8$ for GaNAs/GaAs interface.

interfaces. The second parameter, which is not well known for this system but strongly influences the energy difference between electron levels, is the electron effective mass. We can estimate the difference between electron levels precisely because we observed the $22H$ transition and energies of heavy-hole levels are well known for this system ($h2-h1 \approx 30-35$ meV). Thus, we estimated the energy difference between the second and the first electron levels to be about 75 meV. This difference does not change significantly with the change in the QW depth as it is seen in Fig. 4 (compare solid and dashed lines). On the basis of calculations shown in Fig. 4, we have determined that the electron effective mass in our system is about $0.12m_0$. It corresponds $\sim 100\%$ increase in the electron effective mass in comparison to N free compound, i.e., GaInAsSb. The increase in the electron effective mass is typical of N containing III-V compounds and QW structures.^{42,58-61} Similar electron effective mass has been observed for GaInNAs/GaAs QWs.⁴²

Figure 5 shows calculations of QW transitions for different values of Q_c parameter. On the basis of this figure and literature data,⁶³⁻⁶⁶ we conclude that in our system the acceptable Q_c is in the range of 0.8–0.9 and 0.85–0.90 for GaNAs/GaAs and GaInNAsSb/GaAs interfaces, respectively.

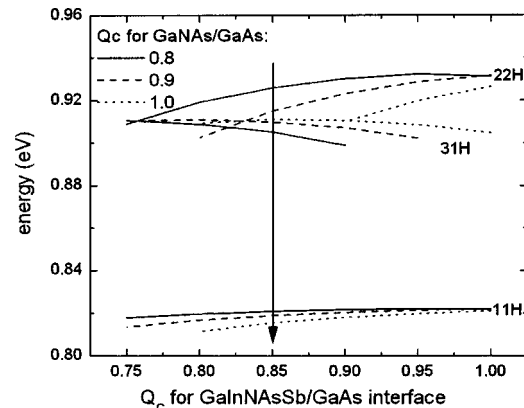


FIG. 5. Energies of QW transitions vs the Q_c for GaInNAsSb/GaAs interface. The solid, dashed and dotted lines correspond $Q_c=0.8, 0.9,$ and $1.0,$ for GaInNAsSb/GaAs interface, respectively.

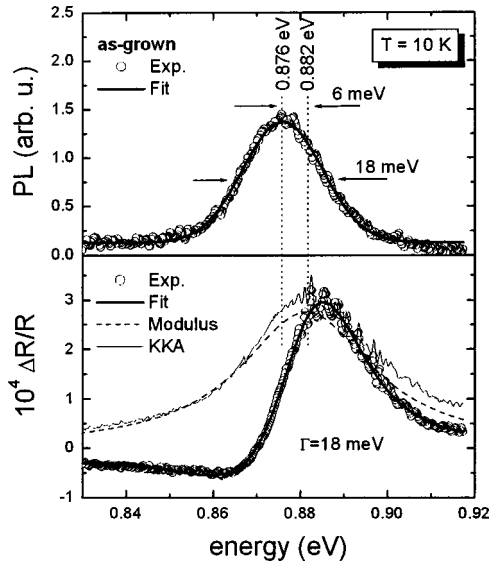


FIG. 6. Comparison of photoluminescence and photoreflectance spectra in the vicinity of the ground state transition for the as-grown GaInNASb/GaNAs/GaAs QW structure.

GaInNAS-based QW structures exhibit specific PL properties at low temperatures. The emission peak of GaInNAS/GaAs QWs is asymmetric with a sharp high-energy cutoff, while the low-energy side has an exponential tail.^{66–69} The tail in this case can be assigned to excitons/carriers, which are localized by potential energy fluctuations near the band edges. The strong carrier localization leads to a large Stokes shift for this system. Note that for GaInNAS/GaAs QWs with smooth interfaces the large Stokes shift is also observed. Therefore, this phenomenon is mainly attributed to unusual properties of GaInNAS alloy. It is expected that an incorporation of Sb atoms into GaInNAS can influence the quality of this material. This issue is carefully investigated in this article.

Figures 6 and 7 show a comparison of PR and PL

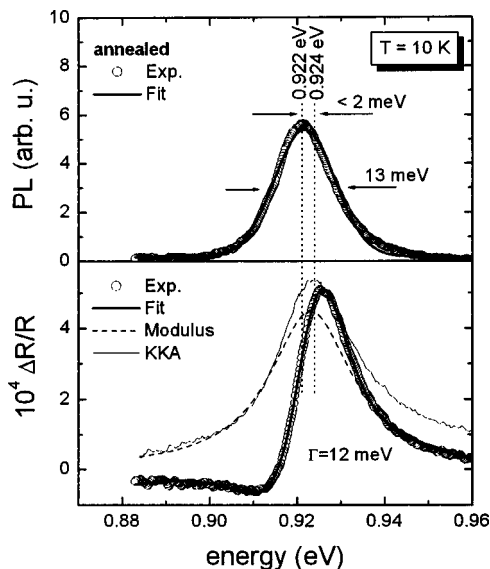


FIG. 7. Comparison of photoluminescence and photoreflectance spectra in the vicinity of the ground state transition for the annealed GaInNASb/GaNAs/GaAs QW structure.

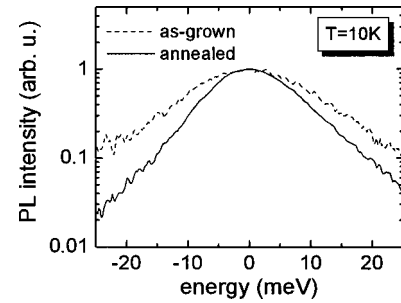


FIG. 8. Comparison of the photoluminescence line shape for the as-grown (dashed line) and annealed (solid line) GaInNASb/GaNAs/GaAs QW structure.

spectra recorded at 10 K for as-grown and annealed GaInNASb/GaNAs/GaAs QW structures, respectively. In order to determine the energy of PR resonance precisely, we have applied the standard fitting procedure assuming Lorentzian line shape with $m=2$ typical of excitonic PR resonance.^{37,70} According to this model PR spectrum can be fitted using the following formula:

$$\frac{\Delta R}{R} = \text{Re}[C e^{i\theta} (\hbar\omega - E + i\Gamma)^{-m}], \quad (3)$$

where $\hbar\omega$ is the photon energy of the probe beam, E is the transition energy, and Γ , C and θ are the broadening, amplitude and phase angle, respectively. The solid and dashed lines in Figs. 6 and 7 are the fit and the modulus of the fit, respectively. In addition, the energy of PR resonance has been determined using KKA, see the thin solid line in Figs. 6 and 7.

We have found that the Stokes shift at 10 K is 6 meV and < 2 meV for as-grown and annealed step-like GaInNASb/GaNAs/GaAs QW structures, respectively. It is much smaller than in typical Ga(In)NAS/GaAs system^{66–69} and could be attributed to the growth process optimization as well as to the introduction of Sb atoms. Probably, the surfactant-like effect of Sb improves the optical quality of the material and it could be the reason for the reduction in carrier localization. Also, the analysis of the line shape of PL peak confirms that the effect of carrier localization is weak in these samples. We observe a symmetric Lorentzian-like peak in Fig. 8 without an exponential tail at the low-energy side, typical of GaInNAS/GaAs QWs. It could be expected that the optical quality would be better for quaternary rather than quinary compound. Additionally, it could be expected that the quality of quaternary/binary interface (GaInNAS/GaAs) should be better than the quality of quinary/ternary interface (GaInNASb/GaNAs). Our results show that good optical quality could be obtained for the QW system composed of quinary compound with quinary/ternary interface, i.e., for the GaInNASb/GaNAs/GaAs QW.

Our experimental results show that this material system has potential applications for high-power edge-emitting lasers (EEL) and vertical-cavity surface-emitting lasers (VCSELs) operating at $1.55 \mu\text{m}$. In the case of the structure reported in this article, the depth of the heavy-hole QW could lead to carrier (hole) leakage problems for the EELs and VCSELs. However, we believe that the depth of the

heavy-hole QW can be easily increased by some modifications in the content of the QW and/or step-like barriers. Sb containing III-V-N compounds will be very promising for optoelectronic devices operating at longer wavelengths.

IV. CONCLUSIONS

Optical properties of the step-like GaInNAsSb/GaNAs/GaAs QW structure were investigated by PR and PL at low and room temperatures. In the case of PR measurements, we have observed optical transitions associated with absorption in the GaInNAsSb/GaNAs/GaAs QW, step-like GaNAs barriers, and GaAs barriers. On the basis of the calculations within the effective mass approximation we have determined the electron effective mass and the band alignment for the GaInNAsSb/GaNAs/GaAs QW as being $m_e \sim 0.12m_0$ and $Q_c \sim 0.85$, respectively. Moreover, we observed the emission peak at 10 K is with small Stokes shift without an exponential tail at the low-energy side. We have observed that the Stokes shift is 6 meV and <2 meV for the as-grown and annealed step-like GaInNAsSb/GaNAs/GaAs QW structure. Hence, we have concluded that the incorporation of Sb atoms into GaInNAs/Ga(N)As QW structure makes it possible to achieve the emission at longer wavelength and helps to keep good optical quality for this system.

ACKNOWLEDGMENTS

This research was supported by the Committee for Scientific Research in Poland under Grant Nos. 4 T11B 008 23 and 2P03B 108 25. Additionally, this work was supported in the United States of America under DARPA and ARO Contract Nos. MDA972-00-1-024, DAAD17-02-C-0101 and DAAD199-02-1-0184, ONR Contract No. N00014-01-1-00100, as well as the Stanford Network Research Center (SNRC). R.K. acknowledges the financial support from the Foundation for Polish Science. H.Y. would like to thank the Stanford Graduate Fellowships for funding assistance.

- ¹M. Kondow, K. Uomi, A. Niwa, T. Kikatan, S. Watahiki, and Y. Yazawa, *Jpn. J. Appl. Phys.*, Part 1 **35**, 1273 (1996).
- ²M. Reinhardt, M. Fischer, M. Kamp, J. Hofmann, and A. Forchel, *IEEE Photonics Technol. Lett.* **12**, 239 (2000).
- ³S. Illek, A. Ultsch, B. Borchert, A. Y. Egorov, and H. Riechert, *Electron. Lett.* **36**, 725 (2000).
- ⁴G. Steinle, H. Riechert, and A. Yu. Egorov, *Electron. Lett.* **37**, 93 (2001).
- ⁵W. Li, T. Jouhti, C. S. Peng, J. Konttinen, P. Laukkanen, E.-M. Pavelescu, M. Dumitrescu, and M. Pessa, *Appl. Phys. Lett.* **79**, 3386 (2001).
- ⁶M. Kawaguchi, T. Miyamoto, E. Gouardes, D. Schlenker, T. Kondo, F. Koyama, and K. Iga, *Jpn. J. Appl. Phys.*, Part 2 **40**, L744 (2001).
- ⁷M. Fischer, D. Gollub, and A. Forchel, *Jpn. J. Appl. Phys.*, Part 1 **41**, 1162 (2002).
- ⁸W. Ha, V. Gambin, M. Wistey, S. Bank, S. Kim, and J. S. Harris, Jr., *IEEE Photonics Technol. Lett.* **14**, 591 (2002).
- ⁹N. Tansu, J.-Y. Yeh, and L. J. Mawst, *Appl. Phys. Lett.* **83**, 2512 (2003), and references therein.
- ¹⁰A. Yue, K. Shen, R. Wang, and J. Shi, *IEEE Photonics Technol. Lett.* **16**, 717 (2004).
- ¹¹J.-M. Hopkins, S. A. Smith, C. W. Jeon, H. D. Sun, D. Burns, S. Calvez, M. D. Dawson, T. Jouhti, and M. Pessa, *Electron. Lett.* **40**, 30 (2004).
- ¹²E. V. K. Rao, A. Ougazzaden, Y. Le Bellego, and M. Juhel, *Appl. Phys. Lett.* **72**, 1409 (1998).
- ¹³Z. Pan, T. Miyamoto, S. Sato, F. Koyama, and K. Iga, *Jpn. J. Appl. Phys.*, Part 1 **38**, 1012 (1999).
- ¹⁴M. Kondow and T. Kitatani, *Semicond. Sci. Technol.* **17**, 746 (2002).
- ¹⁵R. Kudrawiec, G. Sek, J. Misiewicz, L. H. Li, and J. C. Harmand, *Eur.*

- Phys. J.: Appl. Phys.* **27**, 313 (2004).
- ¹⁶J. S. Harris, *Semicond. Sci. Technol.* **17**, 880 (2002), and references therein.
- ¹⁷W. Ha, V. Gambin, M. Wistey, S. Bank, S. Kim, and J. S. Harris, Jr., *Long Wavelength GaInNAs Ridge Waveguide Lasers with GaNAs Barriers*, *Laser and Electro-Optics Society*, 2001, LEOS 2001, The 14th Annual Meeting of the IEEE, Conf. Proc. LEOS 2001, p. 332.
- ¹⁸E.-M. Pavelescu, C. S. Peng, T. Jouhti, J. Konttinen, W. Li, M. Pessa, M. Dumitrescu, and S. Spanulescu, *Appl. Phys. Lett.* **80**, 3054 (2002).
- ¹⁹E.-M. Pavelescu, T. Jouhti, C. S. Peng, W. Li, J. Konttinen, M. Dumitrescu, P. Laukkanen, and M. Pessa, *J. Cryst. Growth* **241**, 31 (2002).
- ²⁰L. F. Bian, D. S. Jiang, S. L. Lu, J. S. Huang, K. Chang, L. H. Li, and J. C. Harmand, *J. Cryst. Growth* **250**, 339 (2003).
- ²¹M. Fischer, D. Gollub, M. Reinhardt, M. Kamp, and A. Forchel, *J. Cryst. Growth* **251**, 353 (2003).
- ²²J. A. Gupta, P. J. Barrios, G. C. Aers, R. L. Williams, and Z. R. Wasilewski, *Solid-State Electron.* **47**, 399 (2003).
- ²³L. H. Li, G. Patriarche, A. Lemaitre, L. Lemaitre, L. Largeau, L. Travers, and J. C. Harmand, *J. Cryst. Growth* **251**, 403 (2003).
- ²⁴H. Y. Liu, M. Hopkinson, P. Navaretti, M. Gutierrez, J. S. Ng, and J. P. R. David, *Appl. Phys. Lett.* **83**, 4951 (2003).
- ²⁵G. Ungaro, G. Le Roux, R. Teissier, and J. C. Harmand, *Electron. Lett.* **35**, 1246 (1999).
- ²⁶J. C. Harmand, G. Ungaro, J. Ramos, E. V. K. Rao, G. Saint-Girons, R. Teissier, G. Le Roux, L. Largeau, and G. Patriarche, *J. Cryst. Growth* **227,228**, 553 (2001).
- ²⁷V. Gambin, W. Ha, M. Wistey, H. Yuen S. R. Bank, S. M. Kim, and J. S. Harris, Jr., *IEEE J. Sel. Top. Quantum Electron.* **8**, 795 (2002).
- ²⁸L. H. Li, V. Sallet, G. Patriarche, L. Largeau, S. Bouchoule, L. Travers, and J. C. Harmand, *Appl. Phys. Lett.* **83**, 1298 (2003).
- ²⁹S. Bank, W. Ha, V. Gambin, M. Wistey, H. Yuen, L. Goddard, S. Kim, and J. S. Harris, *J. Cryst. Growth* **251**, 367 (2003).
- ³⁰K. Volz, V. Gambin, W. Ha, M. A. Wistey, H. Yuen, S. Bank, and J. S. Harris, *J. Cryst. Growth* **251**, 360 (2003).
- ³¹M. A. Wistey, S. R. Bank, H. B. Yuen, L. L. Goddard, and J. S. Harris, Jr., *Electron. Lett.* **39**, 1822 (2003).
- ³²S. R. Bank, M. A. Wistey, L. L. Goddard, H. B. Yuen, V. Lordi, and J. S. Harris, Jr., *IEEE J. Quantum Electron.* **40**, 656 (2004).
- ³³L. H. Li, V. S. Patriarche, L. Largeau, L. Travers, and J. C. Harmand, *J. Cryst. Growth* **263**, 58 (2004).
- ³⁴M. A. Wistey, S. R. Bank, H. B. Yuen, L. L. Goddard, and J. S. Harris, *J. Vac. Sci. Technol. B* **22**, 1562 (2004).
- ³⁵G. M. Peake, K. E. Waldrip, T. W. Hargett, N. A. Modine, and D. K. Serkland, *J. Cryst. Growth* **261**, 398 (2004).
- ³⁶H. B. Yuen, S. R. Bank, M. A. Wistey, A. Moto, and J. S. Harris, Jr., *J. Appl. Phys.* **96**, 6375 (2004).
- ³⁷F. H. Pollak, in *Handbook on Semiconductors*, edited by T. S. Moss (Elsevier, Amsterdam, 1994), Vol. 2, pp. 527–635.
- ³⁸J. Misiewicz, P. Sitarek, G. Sek, and R. Kudrawiec, *Mater. Sci.* **21**, 263 (2003).
- ³⁹S. Jiang, S. C. Shen, S. M. Wang, and T. G. Andersson, *Appl. Phys. Lett.* **66**, 1948 (1995).
- ⁴⁰Y. C. Wang, W. C. Hwang, Z. P. Yang, G. S. Chang, and J. S. Hwang, *Solid State Commun.* **111**, 223 (1999).
- ⁴¹D. J. Hall, T. J. C. Hosea, and C. C. Button, *Semicond. Sci. Technol.* **13**, 302 (1998).
- ⁴²J. Misiewicz, R. Kudrawiec, K. Ryczko, G. Sek, A. Forchel, J. C. Harmand, and M. Hammar, *J. Phys.: Condens. Matter* **16**, 3071 (2004), and references therein.
- ⁴³H. Shen and M. Dutta, *J. Appl. Phys.* **78**, 2151 (1995).
- ⁴⁴R. Kudrawiec, J. Andrzejewski, J. Misiewicz, D. Gollub, and A. Forchel, *International Workshop on Modulation Spectroscopy of Semiconductor Structures*, 1–3 July 2004, Wroclaw, Poland; *Phys. Status Solidi* (in press).
- ⁴⁵T. J. C. Hosea, *Phys. Status Solidi B* **182**, K43 (1994).
- ⁴⁶K. Jezierski, P. Markiewicz, J. Misiewicz, M. Panek, B. Sciana, T. Korbutowicz, and M. Tlaczala, *J. Appl. Phys.* **77**, 4139 (1995).
- ⁴⁷R. Kudrawiec, G. Sek, J. Misiewicz, D. Gollub, and A. Forchel, *Appl. Phys. Lett.* **83**, 2772 (2003).
- ⁴⁸P. J. Klar, H. Grüning, J. Koch, S. Schäfer, K. Volz, W. Stolz, W. Heimbrodt, A. M. Kamal Saadi, A. Lindsay, and E. P. O'Reilly, *Phys. Rev. B* **64**, 121203(R) (2001).
- ⁴⁹R. Kudrawiec, E.-M. Pavelescu, J. Andrzejewski, J. Misiewicz, A. Gheorghiu, T. Jouhti, and M. Pessa, *J. Appl. Phys.* **96**, 2909 (2004).
- ⁵⁰R. Kudrawiec, J. Misiewicz, L. H. Li, and J. C. Harmand, *Solid State*

- Commun. **129**, 353 (2004).
- ⁵¹R. Kudrawiec, E.-M. Pavelescu, J. Wagner, M. Dumitrescu, J. Kontinen, A. Gheorghiu, and M. Pessa, *J. Appl. Phys.* **96**, 2576 (2004).
- ⁵²V. Lordi, V. Gambin, S. Friedrich, T. Funk, T. Takizawa, K. Uno, and J. S. Harris, *Phys. Rev. Lett.* **90**, 145505 (2003).
- ⁵³G. Bastard, *Wave Mechanics Applied to Semiconductor Heterostructures* (Les Editions de Physique, Paris 1992).
- ⁵⁴W. Shan, W. Walukiewicz, J. W. Agger III, E. E. Haller, J. G. Geisz, D. J. Friedman, J. M. Olson, and S. R. Kurtz, *Phys. Rev. Lett.* **82**, 1221 (1999).
- ⁵⁵G. E. Pikus and G. L. Bir, *Sov. Phys. Solid State* **1**, 136 (1960); **1**, 1502 (1960).
- ⁵⁶J. B. Heroux, X. Yang, and W. I. Wang, *J. Appl. Phys.* **92**, 4361 (2002).
- ⁵⁷I. Vurgaftman and J. R. Meyer, *J. Appl. Phys.* **94**, 3675 (2003), and references therein.
- ⁵⁸C. Skierbiszewski, P. Perlin, P. Wisniewski, W. Knap, T. Suski, W. Walukiewicz, W. Shan, K. M. Yu, J. W. Ager, E. E. Haller, J. F. Geisz, and J. M. Olson, *Appl. Phys. Lett.* **76**, 2409 (2000).
- ⁵⁹M. Hetterich, M. D. Dawson, A. Yu. Egorov, D. Bernklau, and H. Riechert, *Appl. Phys. Lett.* **76**, 1030 (2000).
- ⁶⁰Z. Pan, L. H. Li, Y. W. Lin, B. Q. Sun, D. S. Jiang, and W. K. Ge, *Appl. Phys. Lett.* **78**, 2217 (2001).
- ⁶¹G. Baldassarri Höger von Högersthal, P. Polimeni, M. Masia, M. Bissiri, M. Capizi, D. Gollub, M. Fischer, and A. Forchel, *Phys. Rev. B* **67**, 233304 (2003).
- ⁶²S. A. Choulis, T. J. C. Hosea, S. Tomic, M. Kamal Saadi, A. R. Admas, E. P. O'Reilly, B. A. Weinstein, and P. J. Klar, *Phys. Rev. B* **66**, 165321 (2002).
- ⁶³A. Yu. Egorov, V. A. Odnobludov, V. V. Mamutin, A. E. Zhukov, A. F. Tsatsul'nikov, N. V. Kryzhanovskaya, V. M. Ustinov, Y. G. Hong, and C. W. Tu, *J. Cryst. Growth* **251**, 417 (2003).
- ⁶⁴S. Tomic, E. P. O'Reilly, P. J. Klar, H. Gruning, W. Heimbrod, W. M. Chen, and I. A. Buyanova, *Phys. Rev. B* **69**, 245305 (2004).
- ⁶⁵M. Hetterich, A. Grau, A. Yu. Egorov, and H. Reichert, *J. Appl. Phys.* **94**, 1810 (2003).
- ⁶⁶I. A. Buyanova, W. M. Chen, and B. Monemar, *MRS Internet J. Nitride Semicond. Res.* **6**, 2 (2001).
- ⁶⁷E.-M. Pavelescu, T. Jouhti, M. Dumitrescu, P. J. Klar, S. Karirinne, Y. Fedorenko, and M. Pessa, *Appl. Phys. Lett.* **83**, 1497 (2003).
- ⁶⁸E. Tournié, M.-A. Pinault, M. Lüggt, J.-M. Chauveau, A. Trampert, and K. H. Ploog, *Appl. Phys. Lett.* **82**, 1845 (2003).
- ⁶⁹R. Kudrawiec, G. Sek, K. Ryczko, J. Misiewicz, P. Sundgren, C. Asplund, and M. Hammar, *Solid State Commun.* **127**, 613 (2003).
- ⁷⁰D. E. Aspnes, *Surf. Sci.* **37**, 418 (1973).